

Supplementary Information (SI) for Inorganic Chemistry Frontiers.
This journal is © the Partner Organisations 2024

Supporting Information

Heavy Atom engineering of Ru(II) Complex based Sonosensitizers for Enhancing Antifungal Therapy

Qian Li^{a,b,†}, Yida Pang^{b,c,†}, Longcan Mei^{b,†}, Shiming Liang^{d,†}, Huiling Wang^b, Yujia Jiao^e, Sheng Qiu^{a,*}, Hui Chen^{e,*}, Xiwen Xing^{f,*}, and Yao Sun^{b,*}

a. Department of Neurosurgery, Fifth School of Clinical Medicine of Zhejiang Chinese Medical University (Huzhou Central Hospital), Huzhou Key Laboratory of Basic Research and Clinical Translation for Neuromodulation, Huzhou 313099, P. R. China.

b. State Key Laboratory of Green Pesticide, International Joint Research Center for Intelligent Biosensor Technology and Health, College of Chemistry, Central China Normal University, Wuhan 430079, China.

c. Hubei Jiangxia Laboratory, Wuhan 430200, China.

d. National Key Laboratory of Agricultural Microbiology, College of Biomedicine and Health, Huazhong Agricultural University, Wuhan 430070, China.

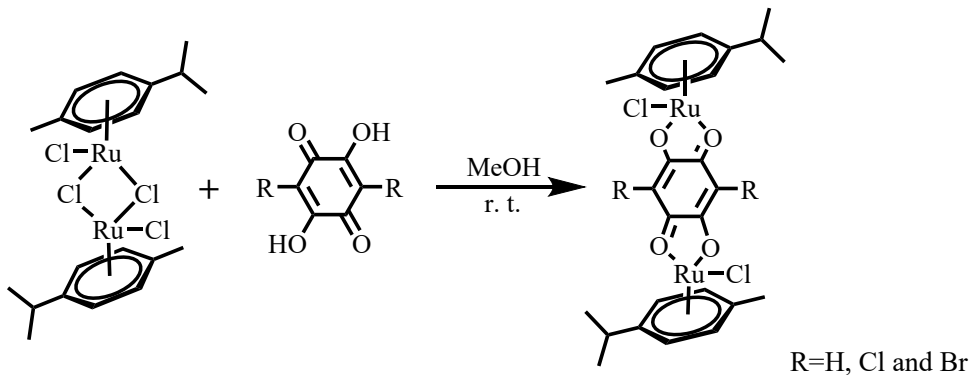
e. Department of Dermatology, Tongji Hospital, Tongji Medical College, Huazhong University of Science and Technology, Wuhan 430030.

f. Department of Biotechnology, College of Life Science and Technology, Jinan University, Guangzhou 510632.

*E-mail address: qius2001@126.com (S. Qiu); chenhui@tjh.tjmu.edu.cn (H. Chen); xingxiwen@jnu.edu.cn (X. Xing); sunyaogbasp@ccnu.edu.cn (Y. Sun).

†Authors contributed equally.

The Synthesis of complexes **RuH**, **RuCl** and **RuBr**.



RuH: Under a nitrogen atmosphere, dissolve dichloro(p-cymene)ruthenium(II) dimer (612.0 mg, 1 mmol, 1 equiv) and 2,5-dihydroxy-1,4-benzoquinone (140.0 mg, 1 mmol, 1 equiv) in 20 mL of anhydrous methanol in a 50 mL round-bottom flask. Stir the reaction mixture at room temperature for 12 h. Afterward, separate the resulting solid using vacuum filtration, and wash the product sequentially with methanol (3×30 mL) and diethyl ether (3×30 mL). Dry the solid under vacuum to collect the red solid **RuH** (610.5 mg, 90.3%). ^1H NMR (400 MHz, CDCl_3) δ 5.91 (s, 2H), 5.74 (d, $J = 5.7$ Hz, 4H), 5.49 (d, $J = 5.6$ Hz, 4H), 3.07 – 2.98 (m, 2H), 2.41 (s, 6H), 1.44 (d, $J = 6.9$ Hz, 12H). ^{13}C NMR (100 MHz, MeOD) δ 184.82, 121.89, 118.83, 101.09, 97.37, 80.81, 78.86, 31.35, 20.93, 17.22. HR-MS is shown in **Fig. S3**: $m/z = 650.334$ for $[\text{M}-\text{Cl}]^+$.

RuCl: Under a nitrogen atmosphere, dissolve dichloro(p-cymene)ruthenium(II) dimer (612.0 mg, 1 mmol, 1 equiv) and chloranilic acid (208.9 mg, 1 mmol, 1 equiv) in 20 mL of anhydrous methanol in a 50 mL round-bottom flask. Stir the reaction mixture at room temperature for 12 hours. Afterward, separate the resulting solid using vacuum filtration, and wash the product sequentially with methanol (3×30 mL) and diethyl ether (3×30 mL). Dry the solid under vacuum to collect the reddish-brown solid **RuCl** (693.7 mg, 93.6%). ^1H NMR (400 MHz, CDCl_3) δ 5.76 (d, $J = 6.1$ Hz, 4H), 5.51 (d, $J = 6.0$ Hz, 4H), 3.08–2.88 (m, 2H), 2.37 (s, 6H), 1.40 (d, $J = 6.9$ Hz, 12H). ^{13}C NMR (100 MHz, MeOD) δ 178.26, 122.42, 118.88, 101.74, 98.17, 81.13, 79.29, 31.68, 21.11, 16.96. HR-MS is shown in **Fig. S7**: $m/z = 718.256$ for $[\text{M}-\text{Cl}]^+$.

RuBr: Under a nitrogen atmosphere, dissolve dichloro-bis(4-methylisopropylbenzene)ruthenium(II) (612.0 mg, 1 mmol, 1 equiv) and bromanilic acid (297.8 mg, 1 mmol, 1 equiv) in 20 mL of anhydrous methanol in a 50 mL round-bottom flask. Stir the reaction mixture at room temperature for 12 h. Afterward, separate the resulting solid using vacuum

filtration, and wash the product sequentially with methanol (3×30 mL) and diethyl ether (3×30 mL). Dry the solid under vacuum to collect the reddish-brown solid **RuBr** (792.3 mg, 95.1%). ^1H NMR (400 MHz, CDCl_3) δ 5.77 (d, $J = 5.8$ Hz, 4H), 5.51 (d, $J = 5.7$ Hz, 4H), 3.05 – 2.87 (m, 2H), 2.39 (s, 6H), 1.43 (d, $J = 6.8$ Hz, 12H). ^{13}C NMR(100 MHz, MeOD) δ 179.24, 121.98, 118.91, 101.89, 97.45, 80.76, 79.29, 31.54, 21.16, 17.24. HR-MS is shown in **Fig. S9**: $m/z = 802.812$ for $[\text{M}-\text{Cl}]^+$.

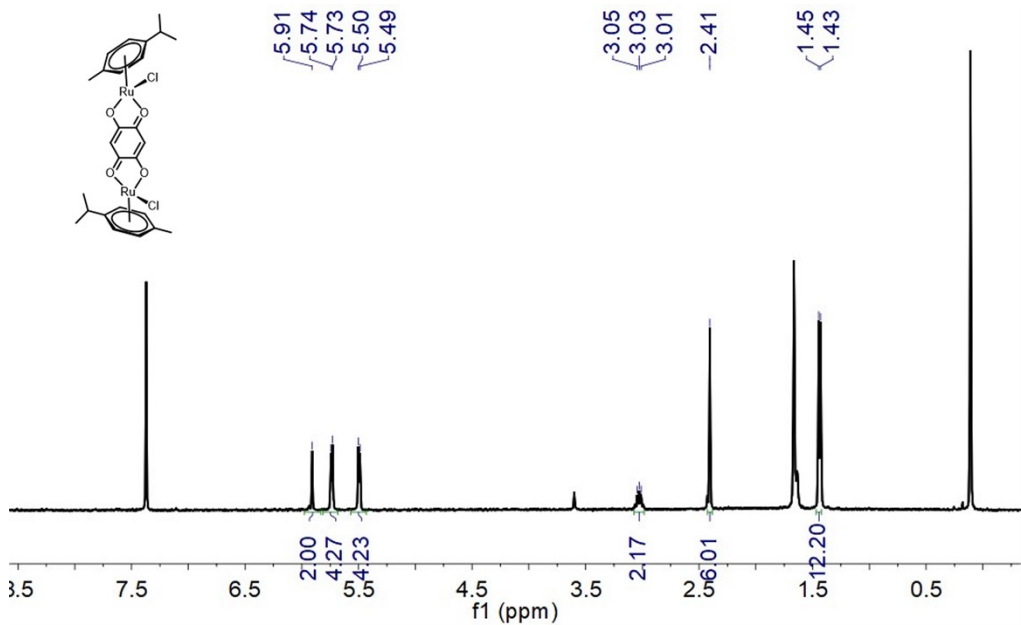


Fig. S1 ¹H NMR spectrum (400 MHz, CDCl₃, 298 K) of **RuH**.

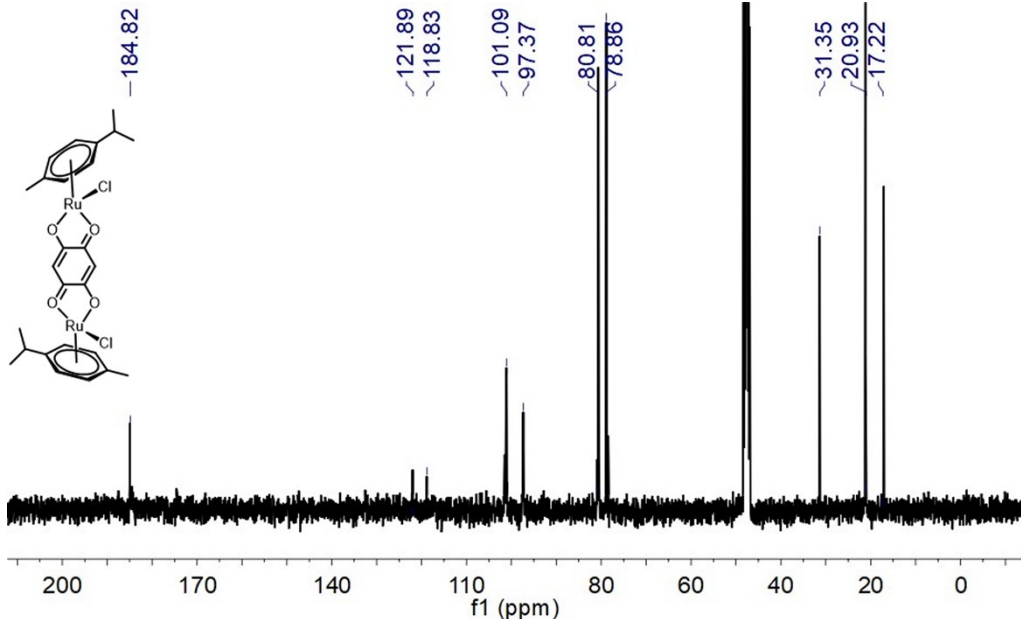


Fig. S2 ¹³C NMR spectrum (100 MHz, MeOD, 298 K) of **RuH**.

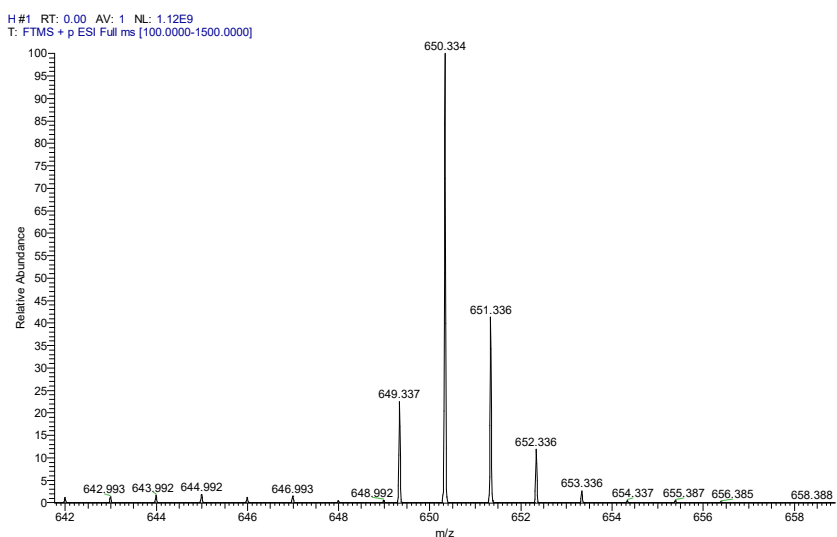


Fig. S3 High-Resolution Mass Spectrometry (HR-MS) spectrum of **RuH**.

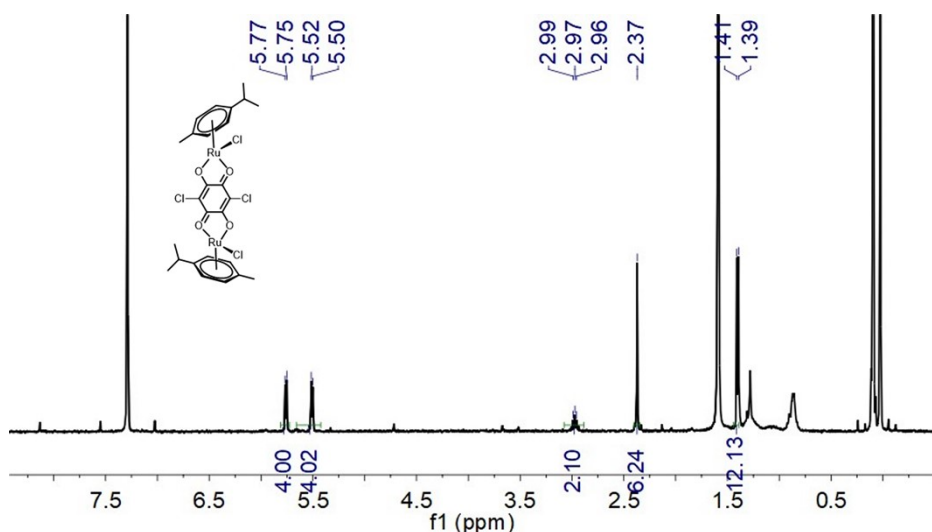


Fig. S4 ^1H NMR spectrum (400 MHz, CDCl_3 , 298 K) of **RuCl**.

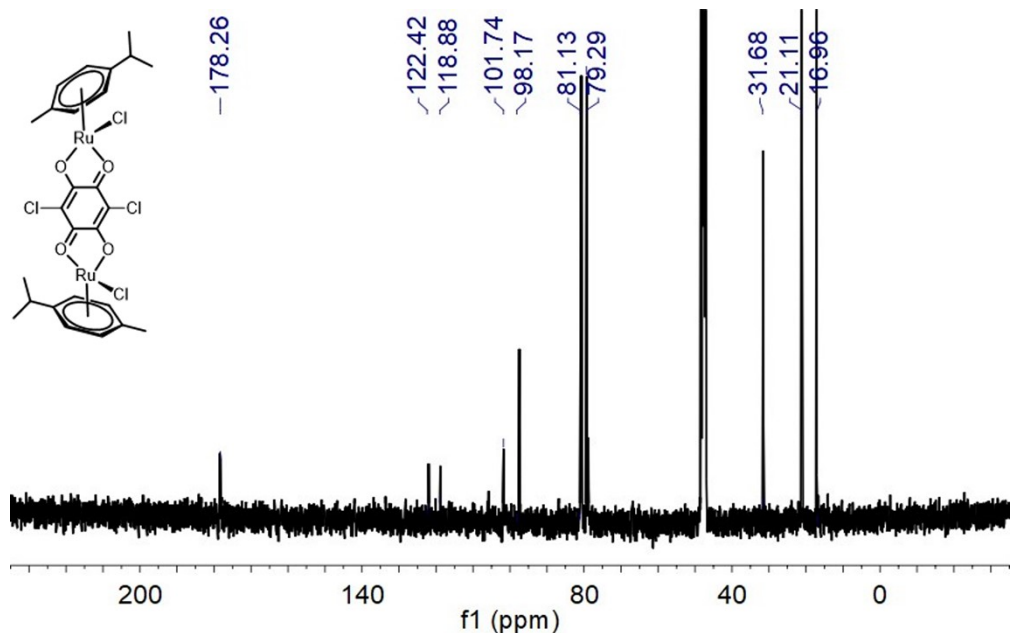


Fig. S5 ^{13}C NMR spectrum (100 MHz, MeOD, 298 K) of **RuCl**.

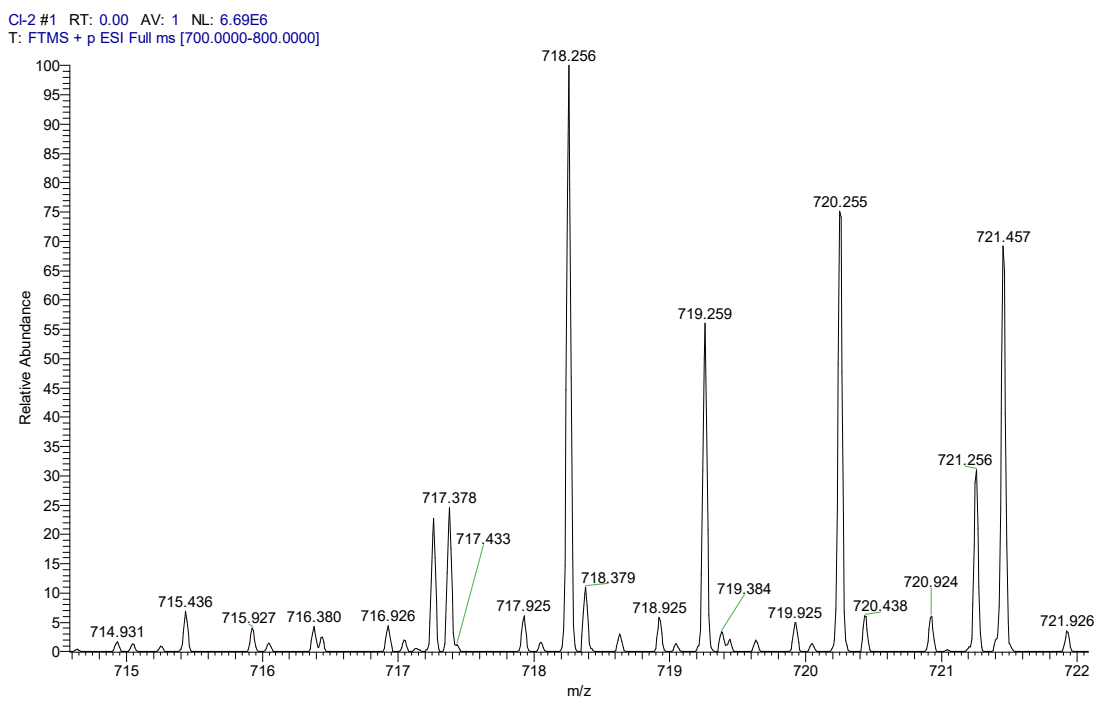


Fig. S6 HR-MS spectrum of **RuCl**.

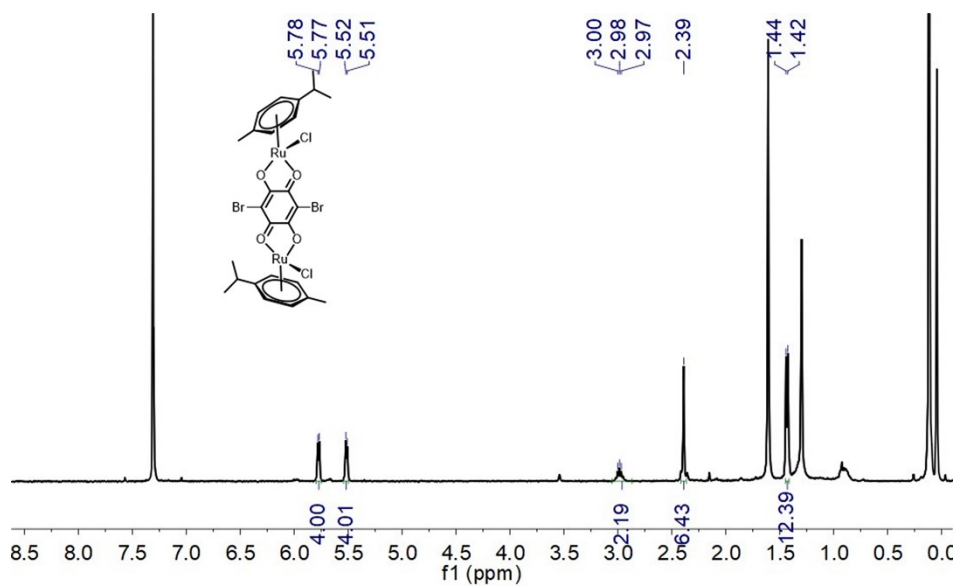


Fig. S7 ^1H NMR spectrum (400 MHz, CDCl_3 , 298 K) of **RuBr**.

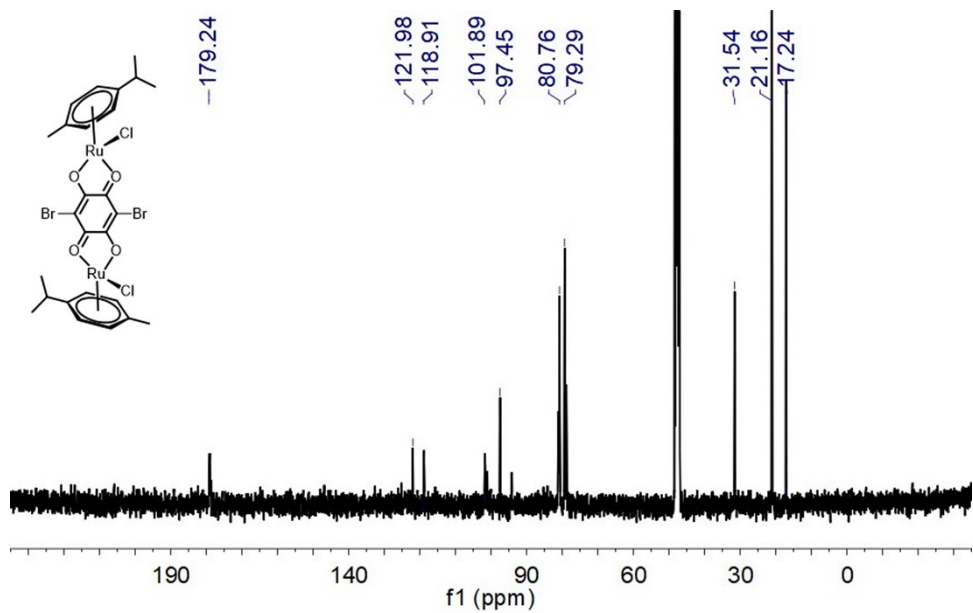


Fig. S8 ^{13}C NMR spectrum (100 MHz, MeOD , 298 K) of **RuBr**.

Br #15 RT: 0.03 AV: 1 NL: 4.92E6
T: FTMS + p ESI Full ms [780.0000-850.0000]

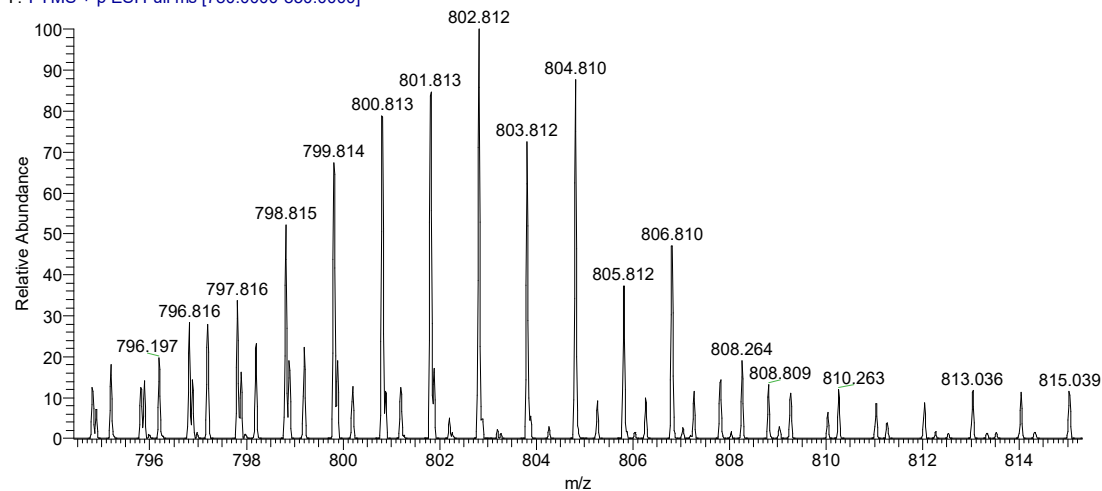


Fig. S9 HR-MS spectrum of RuBr

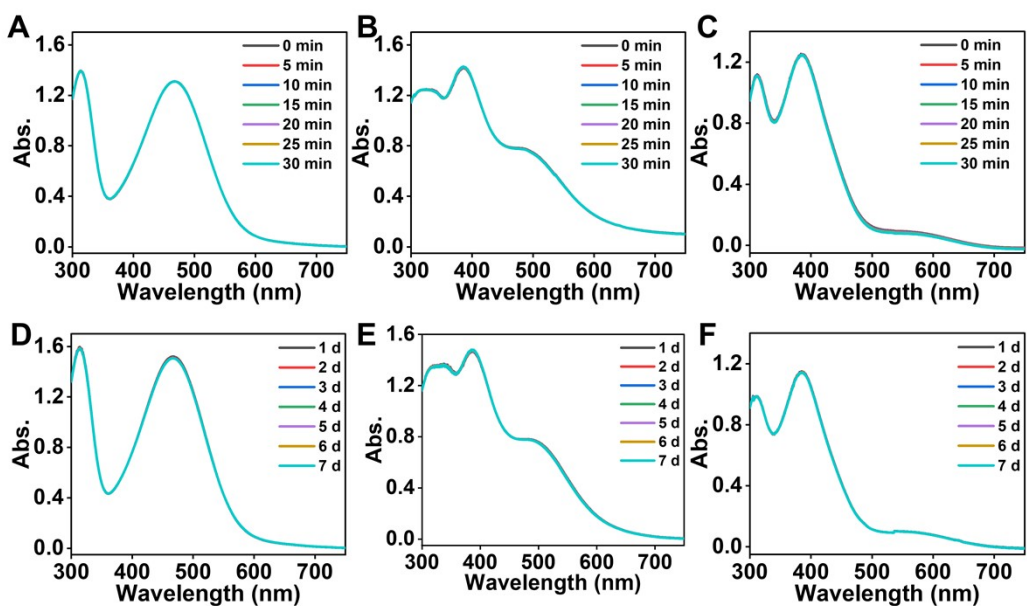


Fig. S10 The stability of **RuH**, **RuCl** and **RuBr** under US irradiation(1 MHz, 50% duty cycle, 1 W/cm²) for 30 min (A) and 7 days in PBS (B).

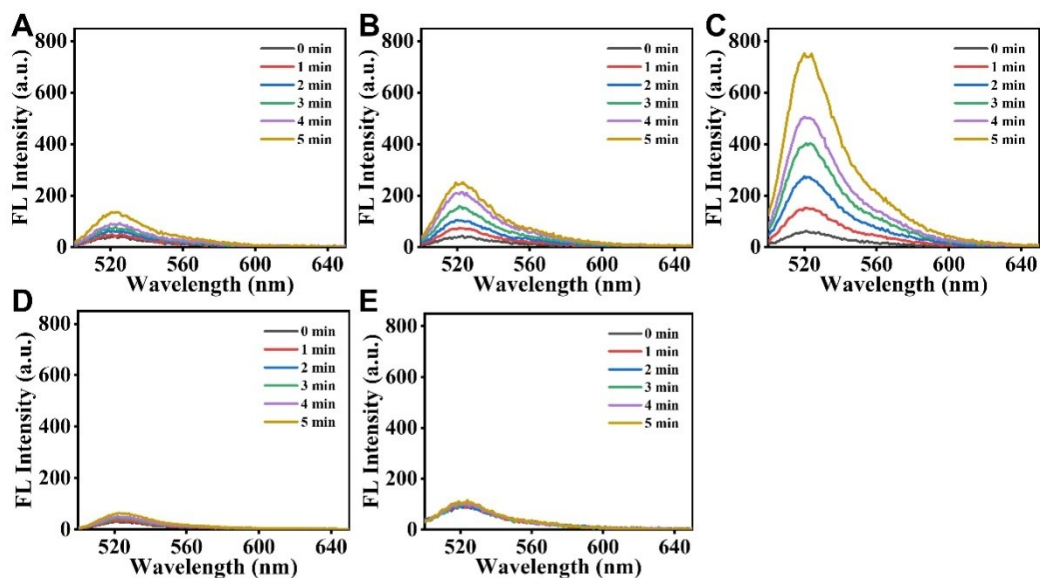


Fig. S11 FL intensity of DCFH by US-activity with **RuH**(A), **RuCl** (B), **RuBr** (C), **Ru(bpy)₃Cl₂** (D) and **H₂O** (E) for 5 min.

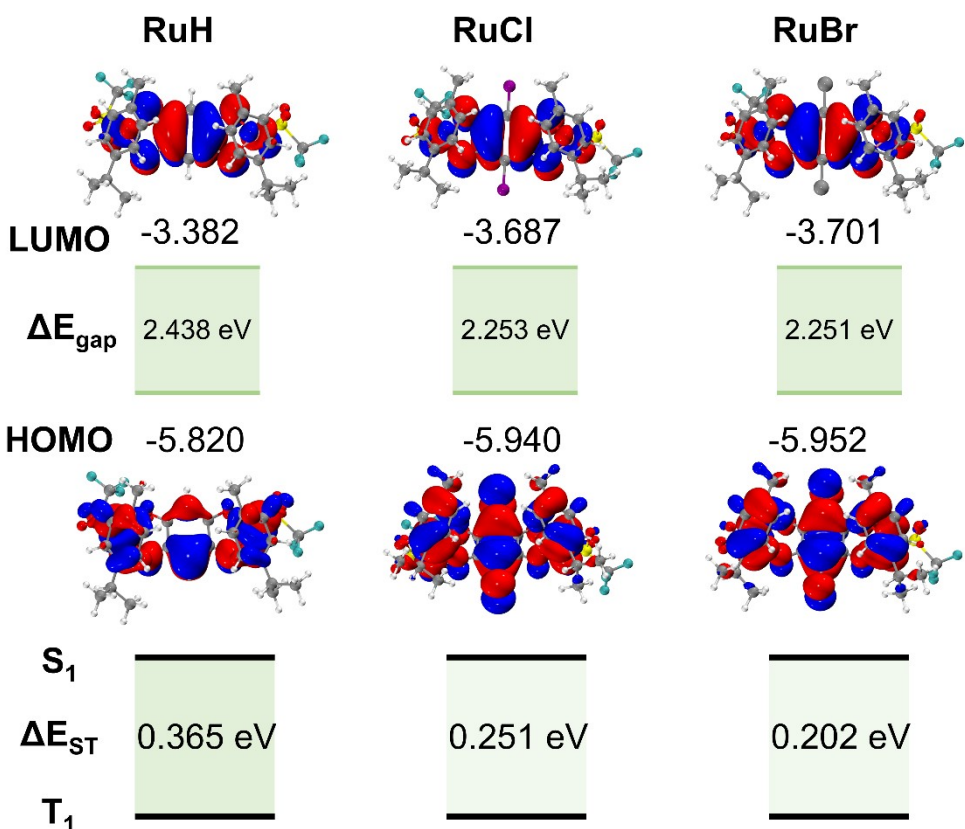


Fig. S12 LUMO, HOMO, E_{gap} and ΔE_{ST} of **RuH**, **RuCl**, **RuBr**.

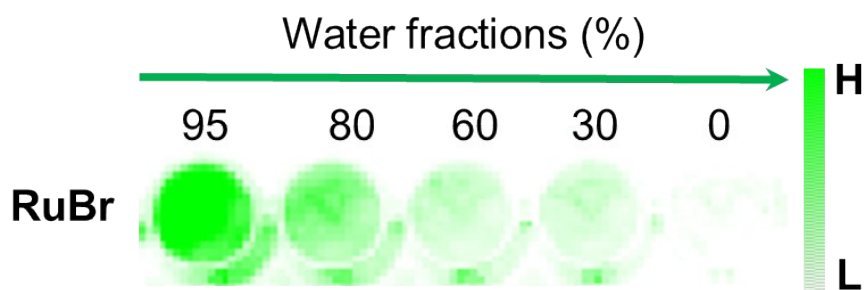


Fig. S13 FL images of DCFH under US irradiation (1 MHz, 50% duty cycle, 1 W/cm², 1 min) with **RuBr** with different water fractions.

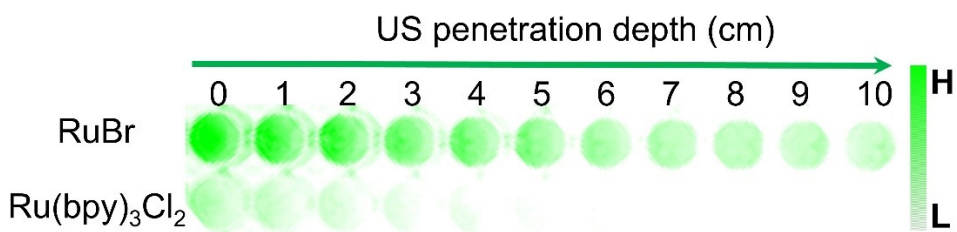


Fig. S14 FL images of DCFH under ultrasound irradiation (1 MHz, 50% duty cycle, 1 W/cm², 1 min) with **RuBr** and **Ru(bpy)₃Cl₂** with different depth of agarose blocks (containing 1% intralipid and 1% agarose).

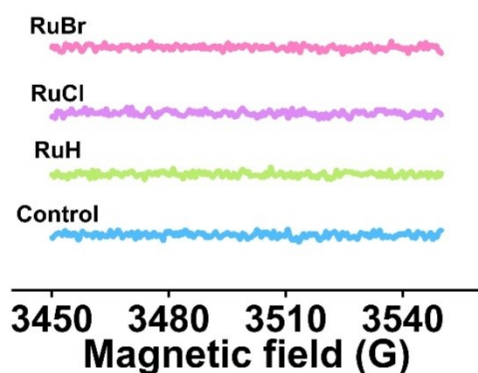


Fig. S15 ESR spectra of **RuH**, **RuCl** and **RuBr** under US irradiation (1 MHz, 50% duty cycle, 1 W/cm², 1 min) with DMPO as capture agent.

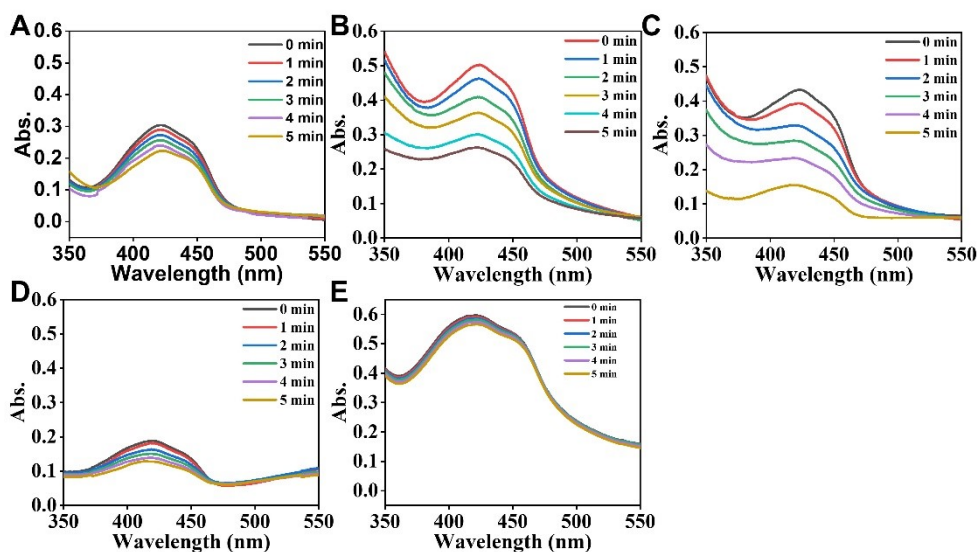


Fig. S16 UV-vis spectrum of DPBF by US-activity (1 MHz, 50% duty cycle, 1 W/cm²) with **RuH** (A), **RuCl** (B), **RuBr** (C), **Ru(bpy)₃Cl₂**(D) and **H₂O** (E) for 5 min.

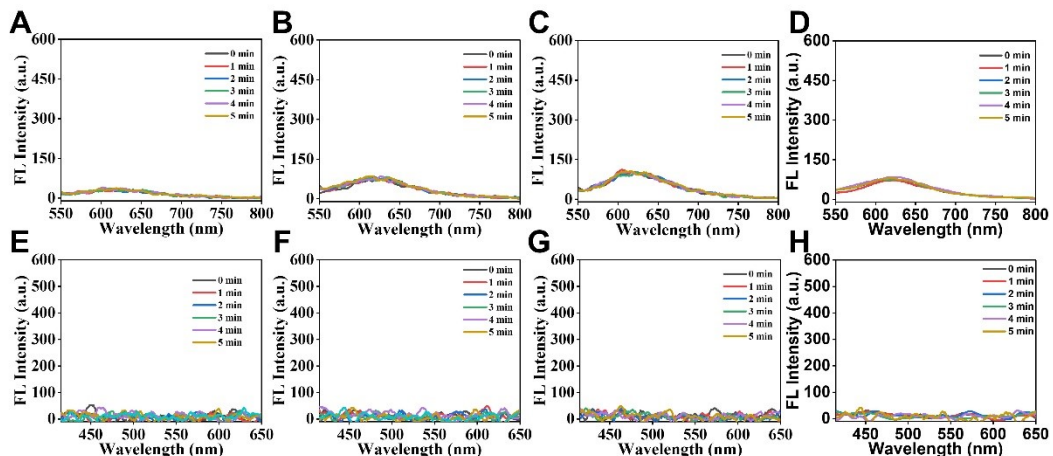


Fig. S17 The detection of O₂⁻ in **RuH** (A), **RuCl** (B), **RuBr** (C) and H₂O (D) solution by using DHE (5 μM) after US irradiation (1 MHz, 50% duty cycle, 1 W/cm², 5 min), λ_{ex} = 488 nm. The detection of •OH in **RuH** (E), **RuCl** (F), **RuBr** (G) and H₂O (H) solution using 3-CCA (5 μM) after US irradiation (1 MHz, 50% duty cycle, 1 W/cm², 5 min), λ_{ex} = 405 nm.

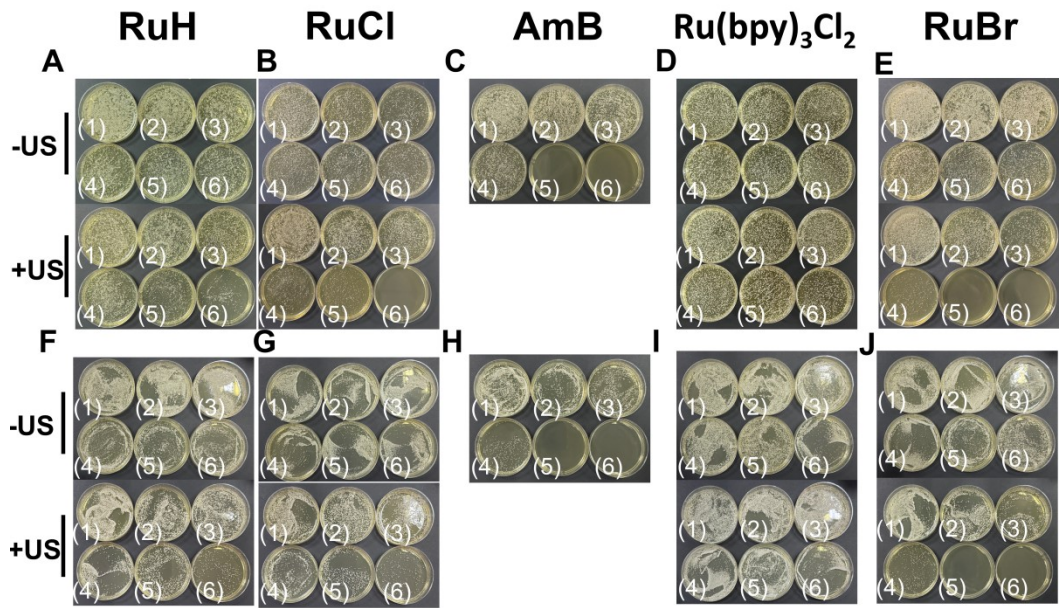


Fig. S18 PA images of *C. albicans* (A-E) and *C. glabrata* (F-J) after incubated with different concentration of **RuH**, **RuCl**, **RuBr**, $\text{Ru}(\text{bpy})_3\text{Cl}_2$ and AmB with/without US irradiation (1 MHz, 50% duty cycle, 1 W/cm²) : 0 μM (1), 2.5 μM (2), 5 μM (3), 10 μM (4), 20 μM (5), 40 μM (6).

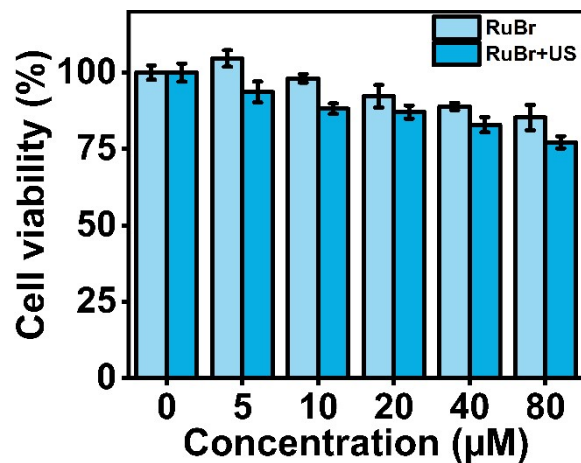


Fig. S19 The relative cellular viability of L929 cells treated with various concentrations of **RuBr** (2.5-40 μM) with/without US irradiation (1 MHz, 50% duty cycle, 1 W/cm², 5 min) (n = 3 independent experiments).

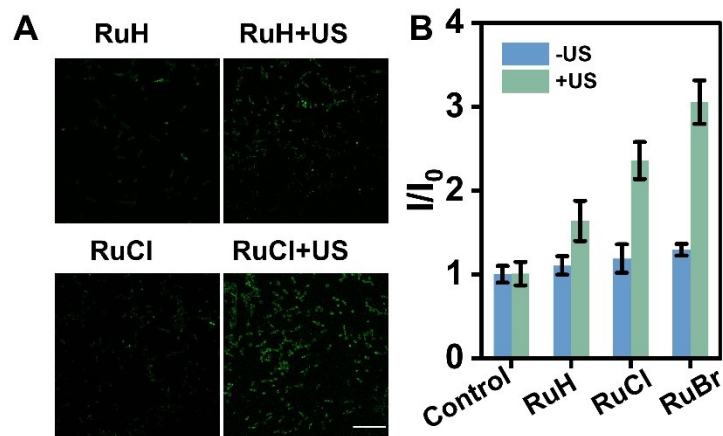


Fig. S20 Fluorescence images (A) and semiquantitative statistics of ROS fluorescence intensity (B) of *C. albicans* stained by DCFH after incubation with **RuH**, **RuCl** and **RuBr**, with or without US irradiation (1 W/cm², 5 min). Scale bar: 20 μ m.

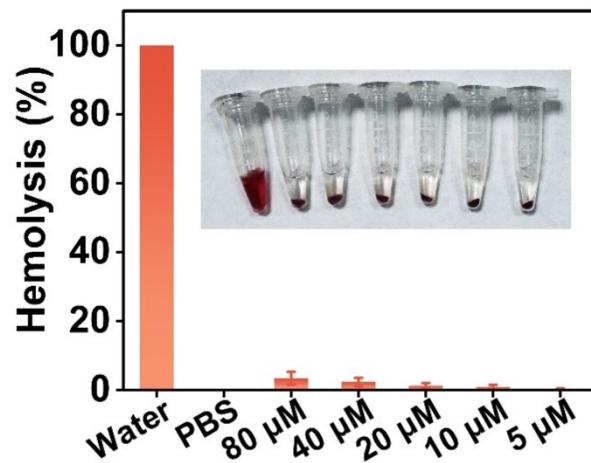


Fig. S21 The hemolysis rate of red blood cells after incubation with different concentrations of **RuBr** (n = 3 independent experiments).



Fig. S22 Schematic of in vivo ultrasound.

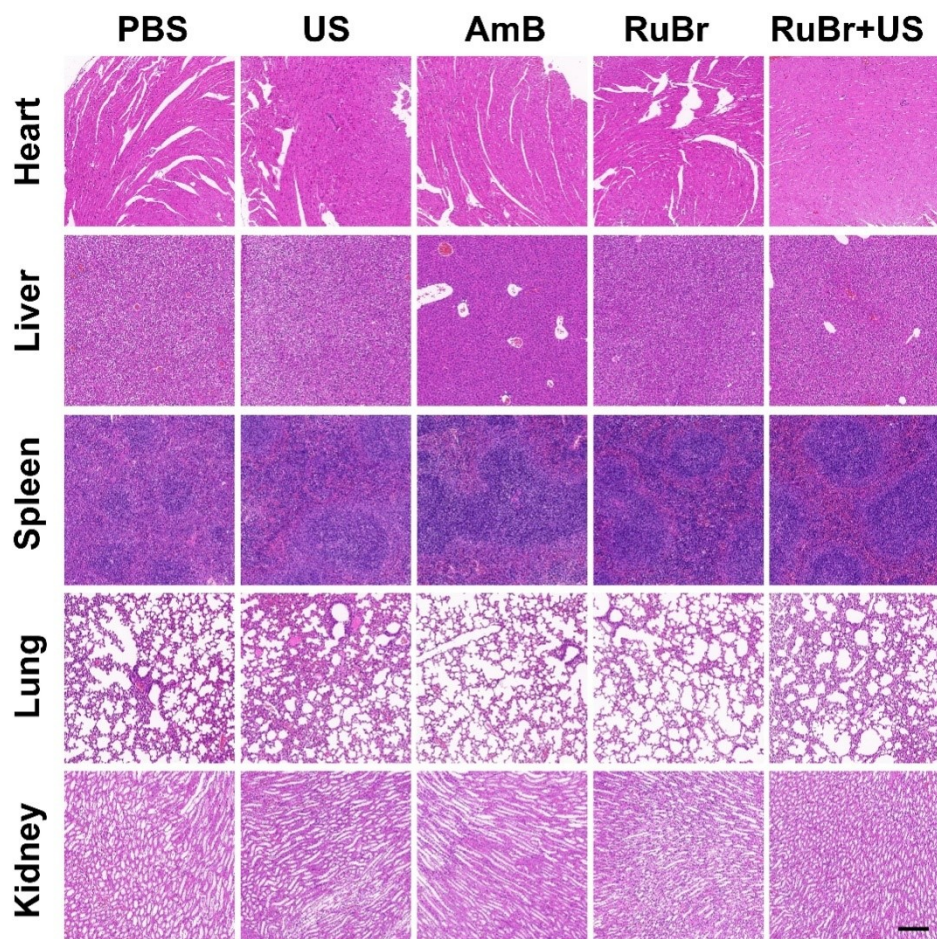


Fig. S23 H&E staining of different organ slices collected from fungi infections mice models at 6 days. Scale bar, 100 μm .